Non-axisymmetric heat flux patterns on tokamak divertor tiles

A. Wingen[1], M.L. Reinke[1], T. Looby[2], D.M. Orlov[3]

[1] *Oak Ridge National Laboratory, Oak Ridge, TN, USA*

[2] *University of Tennessee, Knoxville, TN, USA*

[3] *University of California San Diego, La Jolla, CA, USA*

Non-axisymmetric heat flux patterns on a tokamak divertor can result for several reasons. Two of the most common causes are, first, the plasma equilibrium itself can be non-axisymmetric, either from applied or intrinsic 3D perturbation fields, and second, the plasma facing components (PFCs) may be toroidally asymmetric. Here we introduce a new toolset, called Surface HEat Flux Tracer or SHEFT, that can simulate the heat flux on non-axisymmetric PFCs and is under ongoing development to include 3D plasma equilibrium effects as well. The results presented in this paper are based on axisymmetric plasma equilibria in order to isolate the effects of non-axisymmetric PFCs.

On NSTX-U it has been proposed to use a sawtooth-like profile in the toroidal direction for divertor tiles to shadow leading edges of neighboring tiles from incident heat flux. SHEFT uses a computer assisted drawing (CAD) of the inner wall with all structures, holes and gaps, as well as the shaped divertor tiles.

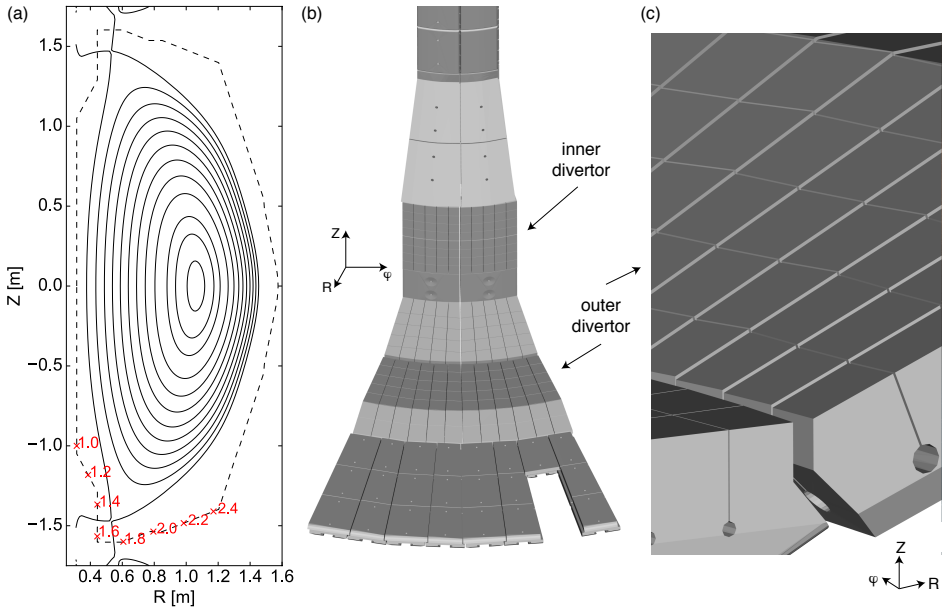

Figure 1: *(a) A poloidal cross-section of the equilibrium. The red numbers indicate S_{wall}, the length along the wall. (b) The CAD of the lower divertor. (c) Magnification of the shaped outer divertor tiles.*

Figure 1(a) shows the setup of the equilibrium, which is based on the up-down symmetric NSTX-U discharge 116313 at 851 ms. The dashed line shows the idealized outline of the wall.

The red markers indicate the S_{wall} coordinate, which measures counter-clockwise the length in meters along the idealized wall, starting at the high-field-side midplane. The CAD of the lower divertor region is shown in Fig. 1(b), while Fig. 1(c) magnifies the outer divertor showing the shaped tiles.

SHEFT works in 3 major steps. In the first step the CAD is used to locate points on top of innermost surfaces. These points are then used in step 2 as initial conditions for tracing. The points are evenly spaced in toroidal angle φ as well as distance along the wall S_{wall}. The relevant constrains are that all points are guarantied to be on top of a CAD surface and that such a surface faces the plasma. The latter implies that the surface normal vector mainly points inwards. This automated process reliably finds all grid points on top of tiles as well as at the bottom of gaps. For now, points along the side walls of tiles inside gaps are not included, as the normal vector of such surfaces typically points away from the plasma. This step is independent of the plasma equilibrium and can be run once up front to determine and store the initial conditions. On 20 cores it takes less than a minute to generate a 600×400 grid.

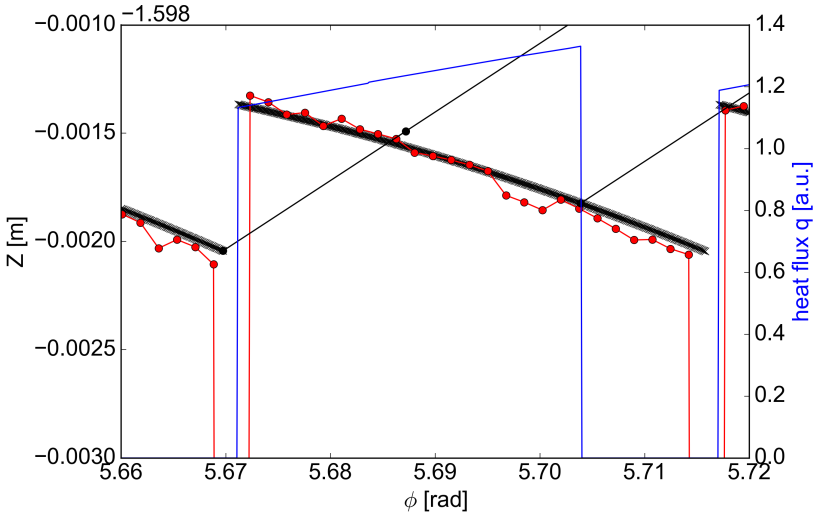

Figure 2: *Initial conditions and shadow effect along the shaped tiles of the outer divertor: (black marker) grid points along the tile surface, (red marker and lines) low resolution wall outline, (blue line) incident heat flux profile, (black lines) field lines launched from the tile surface.*

In step 2 the MAFOT code [1] traces field lines, using the points from step 1 as initial conditions, back into the scrape-off layer (SOL) and plasma. In general the MAFOT code can trace magnetic field lines as well as guiding center particle drift orbits in 3D magnetic configurations which, based on an EFIT equilibrium, can include intrinsic or applied 3D fields as well as MHD plasma response solutions. MAFOT is fully parallel, while the run time depends on the grid size as well as the complexity of the equilibrium. Here we only use axisymmetric EFIT equilibria,

so the trace of a 600×400 grid is completed in about 60 s on 20 cores. The trace returns the minimum penetration depth ψ_{min} in terms of normalized poloidal flux of each field line. In an axisymmetric equilibrium this is quite trivial, as field lines remain on nested surfaces of constant flux. In 3D magnetic configurations this is no longer the case though. One important element of this step is to terminate field lines which intersect with other parts of the CAD wall in order to simulate the shadow effect of neighboring tiles.

The black markers in Fig. 2 are the high resolution initial conditions, as obtained in step 1, along a few tiles of the outer divertor. The sawtooth-like shaping with toroidal angle is obvious. The red markers and line represent a low resolution outline of the wall, obtained from the CAD, which is only used in the MAFOT code as boundary condition for field line termination. Two example field lines, given by the black lines, are launched from the tile surfaces. The first one at the very corner of the left tile (near $\varphi = 5.67$), the second one from the center tile near $\varphi = 5.704$. Both field lines intersect with other parts of the CAD wall within the first integration step of the trace. The second field line just barely touches the corner of the tile on the right. So, the points on the tile for both field lines should not register any incident heat flux. The blue line shows the resulting heat flux profile, which drops to zero for areas that are shadowed by neighboring tiles. The second field line was launched from the first point that is shadowed by the right tile. All further points towards the right are also shadowed.

In step 3 heat flux is assigned to the penetration depth ψ_{min} via a predefined profile (see [2])

$$q(R(\psi)) = \frac{q_0}{2} \exp\left[\left(\frac{S}{2\lambda_q}\right)^2 - \frac{R-R_s}{\lambda_q}\right] \operatorname{erfc}\left(\frac{S}{2\lambda_q} - \frac{R-R_s}{S}\right) + q_{BG}. \quad (1)$$

with $R(\psi)$ the major radius at the outer midplane as function of normalized poloidal flux, and R_s the major radius of the separatrix on the low-field-side. Here we are assuming an Eich profile [2], using the heat flux layer width λ_q, the spreading S into the private flux region and the total power delivered to each divertor target. Figure 3 shows the profile of the incident heat flux along the inner divertor, which is based on Eq. (1). The profile is interrupted by two spikes. They are the result of gaps between tiles. Inside the gaps the heat flux typically drops to zero, because field lines launched from the bottom usually intersect with neighboring tiles. The gaps are shad-

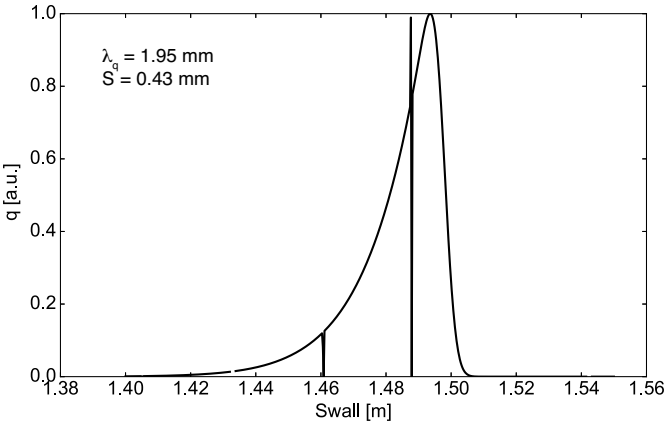

Figure 3: *Incident heat flux profile along the inner divertor for a fixed toroidal angle.*

owed. For the gap near $S_{wall} = 1.488$ a spike larger than the surrounding profile is registered. In such a case, field lines from the bottom of the gap connect into the SOL, which means heat flux can reach the bottom of that gap. Due to an increased incident angle, which is given as $\vec{n} \cdot \vec{B}/|B|$ for the surface normal vector $\vec{n}$ and the magnetic field vector $\vec{B}$, the heat flux is larger in the gap than on the top surface of surrounding tiles.

The final result, the heat flux pattern on the divertor surface, is shown in Fig 4 for the lower inner divertor (a) and the lower outer divertor (b). The inner divertor surface is mostly axisymmetric, except for the gaps, resulting in an toroidally even distribution of heat flux. The outer divertor shows the effect of the shaped tiles which shadow adjacent tiles for $S_{wall} > 1.8$. Furthermore, the shaped tiles are slightly tilted, so that the incident angle is not constant across the tile, resulting in a toroidal heat flux gradient within the tiles. SHEFT has been successfully tested against multiple NSTX-U equilibria, including single and double null geometries. Although MAFOT can simulate 3D equilibria in Step 2, a model for assigning heat flux to stochastic field lines inside the lobes of perturbed footprints needs to be added in Step 3. A model based on ion drift orbits [3] is under ongoing development. The drift model will be added to the new toolset in the future. The tool will also be combined with a recently developed code that computes surface heat flux from measurements of sub-surface thermocouples, using machine learning. This work is supported by the US Department of Energy under DE-AC05-00OR22725, DE-AC02-09CH11466 and DE-FG02-05ER54809.

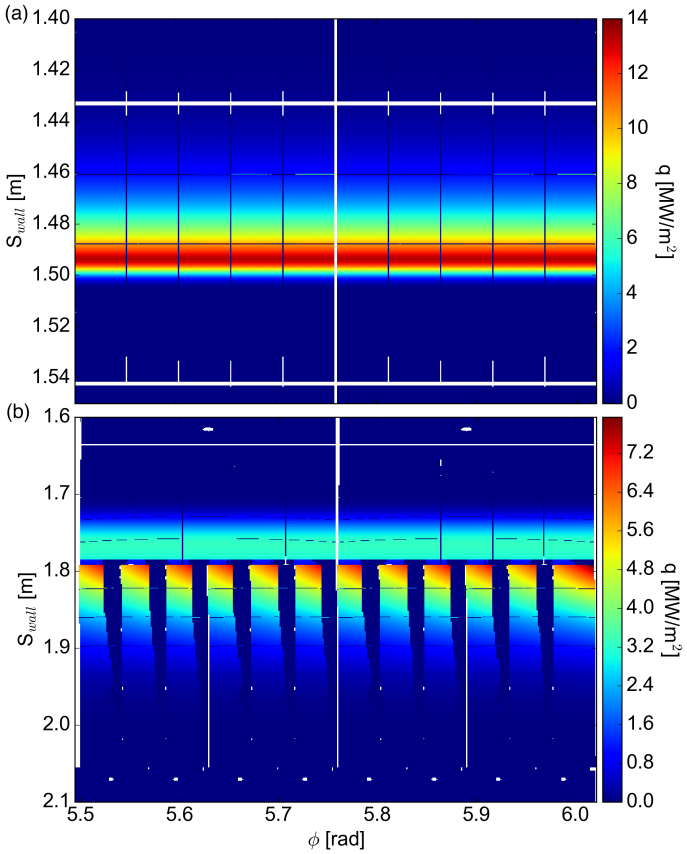

Figure 4: *Simulated incident heat flux on NSTX-U lower (a) inner and (b) outer divertor for discharge 116313 at 851 ms. The white areas are holes in the wall's CAD model.*

References

[1] A. Wingen, T. E. Evans, and K. H. Spatschek, Nuclear Fusion **49**, 055027 (2009).

[2] T. Eich *et al.*, Physical Review Letters **107**, 215001 (2011).

[3] A. Wingen, O. Schmitz, T. E. Evans, and K. H. Spatschek, Physics of Plasmas **21**, 012509 (2014).